nature structural & molecular biology

Phospholipid-dependent regulation of the motor activity of myosin X

Nobuhisa Umeki[1,3], Hyun Suk Jung[2,3], Tsuyoshi Sakai[1,3], Osamu Sato[1], Reiko Ikebe[1] & Mitsuo Ikebe[1]

Myosin X is involved in the reorganization of the actin cytoskeleton and protrusion of filopodia. Here we studied the molecular mechanism by which bovine myosin X is regulated. The globular tail domain inhibited the motor activity of myosin X in a Ca^{2+}-independent manner. Structural analysis revealed that myosin X is monomeric and that the band 4.1-ezrin-radixin-moesin (FERM) and pleckstrin homology (PH) domains bind to the head intramolecularly, forming an inhibited conformation. Binding of phosphatidylinositol-3,4,5-triphosphate (PtdIns(3,4,5)P_3) to the PH domain reversed the tail-induced inhibition and induced the formation of myosin X dimers. Consistently, disruption of the binding of PtdIns(3,4,5)P_3 attenuated the translocation of myosin X to filopodial tips in cells. We propose the following mechanism: first, the tail inhibits the motor activity of myosin X by intramolecular head-tail interactions to form the folded conformation; second, phospholipid binding reverses the inhibition and disrupts the folded conformation, which induces dimer formation, thereby activating the mechanical and cargo transporter activity of myosin X.

Myosin X is ubiquitously expressed in a variety of cell types[1]. As is common to all members of the myosin superfamily, myosin X has a conserved motor domain in its N-terminal region, and this is followed by three isoleucine-glutamine (IQ) motifs that serve as light-chain binding sites (**Fig. 1**). After the IQ domain there is a predicted coiled-coil domain, and it was originally thought that myosin X was a two-headed myosin. However, a recent study revealed that the proximal part of the coiled-coil domain does not form a coiled coil but rather a rigid single α-helix (SAH)[2]. The C-terminal globular tail domain (GTD) is composed of several subdomains: a PEST domain, three PH domains, a myosin tail homology 4 (MyTH4) domain and a FERM domain[1]. The tail domain was reported to bind to specific cargo molecules[3–5]. As myosin X moves toward the tips of filopodia and transports cargo molecules, it was thought to function as a cargo carrier. Consistent with these findings, it was shown that myosin X is a plus-end–directed, high-duty-ratio myosin[6,7] in which the head spends most of its cross-bridge cycle time in strong-actin-binding form. It is therefore suitable for 'processive' movement[8,9], and the tail-truncated myosin X forced dimer can move processively on single actin filaments[10]. Myosin X continuously moves in filopodia at the single-molecule level[11,12]. Although myosin X has been found to be discretely localized at the tip of filopodia[13], a substantial amount of myosin X is found in the cytosol without any notable specific localization[14]. This suggests that the cargo-transporting function of myosin X is regulated and that the myosin X molecules in filopodia are activated to move to the tip, whereas myosin X in the cell body is inactivated. We therefore set out to clarify the regulation mechanism of the myosin X motor and cargo-transporting function.

We found here that the full-length myosin X (M10full) is monomeric and that the tail domain interacts directly with the motor domain to form a folded structure that results in the inhibition of the actin-activated ATP hydrolysis cycle. Phospholipid binding at the PH domain in the tail abolishes the inhibition and induces the activation of the ATP hydrolysis cycle and dimer formation, which leads to the activation of the cargo-transporter function of myosin X.

RESULTS

Full-length myosin X is monomeric

We produced a series of truncated myosin X constructs to study the regulation mechanism (**Fig. 1**). We co-purified the isolated myosin X heavy chain with calmodulin light chain (CaM; **Supplementary Fig. 1**). The apparent molecular masses of the truncated myosins, as determined from SDS-PAGE mobility, were 235 kDa, 120 kDa, 140 kDa and 90 kDa for M10full and three truncated versions, M10ΔGTD, M10M5cc and M10IQ0, respectively. These values agree well with the calculated molecular masses expected for these constructs.

Electron microscopy studies have concluded that the tail-truncated myosin X (M10ΔGTD) is predominantly a monomer[2]. Consistent with this observation, we found that almost no M10ΔGTD was cross-linked to form a dimer. This is in contrast to M10M5cc, which has the coiled coil of myosin Va and forms a stable dimer (**Supplementary Fig. 2a**).

An important question is whether the tail domain influences the stability of myosin X dimer formation. We subjected M10full to chemical cross-linking and detected essentially no dimers, in contrast to M10full LZ, which has a C-terminal leucine zipper module (**Supplementary Fig. 2b**). The results suggest that the tail domain does not promote the formation of myosin X dimers (**Supplementary Fig. 2b**). Negative-staining electron microscopy revealed that M10full formed single-headed

[1]Department of Microbiology and Physiological Systems, University of Massachusetts Medical School, Worcester, Massachusetts, USA. [2]Division of Electron Microscopic Research, Korea Basic Science Institute, Daejeon, Korea. [3]These authors contributed equally to this work. Correspondence should be addressed to M.I. (Mitsuo.Ikebe@umassmed.edu).

Received 8 August 2010; accepted 1 April 2011; published online 12 June 2011; doi:10.1038/nsmb.2065

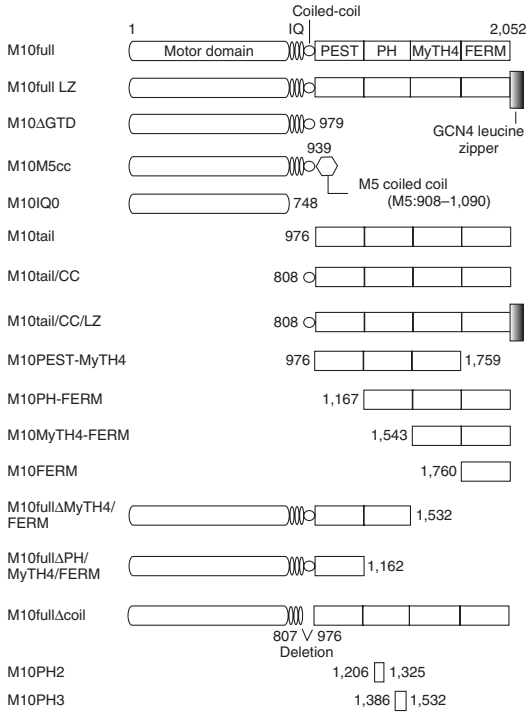

Figure 1 Schematic diagram of myosin X constructs used in this study. Amino acid numbers of the constructs are indicated.

structures with a pear-like appearance (see **Supplementary Fig. 3**). These results indicate that full-length myosin X is monomeric.

The myosin X tail inhibits motor activity

The actin-activated ATPase activity of myosin X showed hyperbolic saturation characteristics for both M10full and M10ΔGTD (**Fig. 2**) to yield values of V_{max} and K_{actin} (the actin concentration that provides a half V_{max}) as shown in **Table 1**. The V_{max} of M10full was Ca^{2+} independent and much lower than that of M10ΔGTD under both high and low Ca^{2+} conditions. K_{actin} values were also not influenced by Ca^{2+} for M10full or M10ΔGTD, although the values were approximately two-fold higher for M10ΔGTD. The K_{actin} value for M10ΔGTD here was approximately three-fold higher than that previously obtained for the M10IQ1 construct[7]. This might be due to the presence of the distal IQ and proximal tail region of M10ΔGTD or to the difference in the ionic conditions used. This result suggests that the tail domain of myosin X inhibits the actin-activated ATPase activity. Consistent with this idea, the tail domain (M10tail) markedly inhibited the actin-activated ATPase activity of M10ΔGTD, regardless of Ca^{2+} concentration (**Fig. 2b**). The inhibition of ATPase activity was dose dependent, and the apparent affinity between M10ΔGTD and the tail domain was 0.85 μM (**Fig. 2b**). M10tail (0.5 μM) decreased V_{max} and slightly increased K_{actin} (to 12.9 ± 3.7 s^{-1} and 68.9 ± 15.4 μM, respectively; **Supplementary Fig. 4a**). The actin-activated ATPase activity of myosin Va and myosin VIIa is inhibited by their tail domains at low Ca^{2+}, but not inhibited at high Ca^{2+} (refs. 15,16). By contrast, the inhibition of M10ΔGTD by the tail domain was independent of Ca^{2+}. The result suggests that the tail of myosin X inhibits its activity by a different mechanism from that of myosin Va or myosin VIIa.

Although myosin X was predominantly a monomer, it is plausible that myosin X forms a dimer in cells and that this could alter the regulation of the ATPase activity. The ATPase activity of M10M5cc, a forced dimer, was also markedly inhibited by M10tail (**Supplementary Fig. 4b**). The apparent affinity between M10tail and M10M5cc was 1.08 μM, a value similar to that for M10ΔGTD. These results indicate that dimer formation does not influence the tail-induced inhibition of myosin X. The tail also attenuated the basal ATPase activity (**Supplementary Fig. 4c**). The inhibition of myosin X by its tail showed significant dependence on salt concentration, being more profound with concentrations of KCl less than 200 mM (**Supplementary Fig. 5**). These results suggest that the inhibition depends on an ionic interaction between the tail domain and the head-neck domain of myosin X.

The key regions for tail inhibition of myosin X

We produced a series of truncation mutants of myosin X (**Fig. 1**) to determine which sites were crucial for the tail-induced inhibition of ATPase activity. The deletion of the FERM domain (M10PEST-MyTH4) abolished the inhibitory activity of the tail (**Fig. 2c**). In contrast, deletion of the N-terminal PEST domain (M10PH-FERM) did not affect the inhibitory activity (**Fig. 2c**). Further truncation of the PH domain abolished the inhibitory activity of the tail (**Fig. 2c**). These results suggest that both the PH and FERM domains of the tail are required for the inhibition and that both are important for the binding of the tail domain to M10ΔGTD.

However, the elimination of both IQ domains and the SAH–coiled-coil domain from M10ΔGTD had no effect on tail-induced inhibition (**Fig. 2d**). Furthermore, M10IQ0 co-immunoprecipitated with M10PH-FERM (**Fig. 2d**, inset). This is quite different from the cases of myosin Va and myosin VIIa[15,16], in which the deletion of the coiled-coil domain and the distal IQ domains, respectively, abolished the

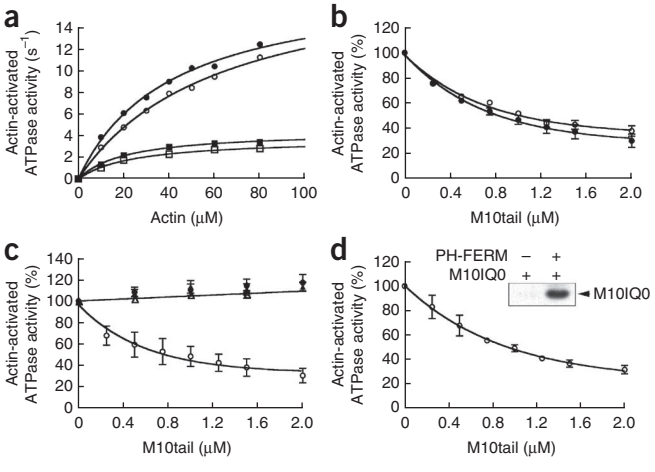

Figure 2 The actin-activated ATPase activity of M10full and M10ΔGTD. (**a**) Actin-activated ATPase activity of M10full is much lower than of M10ΔGTD. The ATPase activity was measured as described in the Online Methods. Open circles, M10ΔGTD in pCa4; closed circles, M10ΔGTD in EGTA; open squares, M10full in pCa4; closed squares, M10full in EGTA. (**b**) Inhibition of the actin-activated ATPase activity of M10ΔGTD by exogenous tail domain. Assay conditions are as described in Online Methods. Values are mean ± s.e.m. from three independent experiments. Closed circles, EGTA; open circles, pCa4. One hundred percent activities in EGTA and pCa4 conditions were 5.83 ± 0.24 s^{-1} and 4.42 ± 0.36 s^{-1}, respectively. (**c**) Determination of the regions in the tail domain that are crucial for inhibition of the actin-activated ATPase activity of M10ΔGTD under EGTA conditions. Open circles, M10PH-FERM; closed circles, M10PEST-MyTH4; open triangles, M10MyTH4-FERM; closed triangles, M10FERM. One hundred percent represents 5.83 ± 0.24 s^{-1}. (**d**) Effect of M10tail on the actin-activated ATPase activity of M10IQ0 under EGTA conditions. One hundred percent represents 6.59 ± 0.32 s^{-1}. Inset shows the pulldown assay (see **Supplementary Methods**). Values are mean ± s.e.m. from three independent experiments.

Table 1 The V_{max} and K_{actin} values of actin-activated ATPase activity of M10full and M10ΔGTD with or without Ca^{2+}

		V_{max} (s^{-1})	K_{actin} (μM)
M10full	EGTA	4.27 ± 0.32	21.73 ± 2.58
	pCa4	3.58 ± 0.18	22.40 ± 2.35
M10ΔGTD	EGTA	20.07 ± 1.64	46.87 ± 6.68
	pCa4	19.59 ± 2.35	59.41 ± 8.42

All data are presented as mean ± s.d. (n = 3 from three independent preparations of each construct).

tail-induced inhibition. These results indicated that the tail domain (PH-FERM) directly interacts with the motor domain to inhibit the actin-activated ATPase activity.

Visualization of inhibited form of myosin X

We performed negative staining followed by single-particle analysis to clarify the structural basis of the tail inhibition mechanism of myosin X (**Fig. 3**). Images of M10IQ0 showed single-headed molecular shapes (**Fig. 3a**). They appeared to show the head without the IQ domain with a length of 12–13 nm and a width of 5–6 nm (**Fig. 3e** and **Supplementary Fig. 3d**). Consistent with previous findings[2], M10ΔGTD molecules were predominantly monomeric (**Fig. 3b**), adopting pear-like shapes for the head with a length of 14–17 nm and a width of 5–6 nm (**Fig. 3e** and **Supplementary Fig. 3d**). In the presence of exogenous tail domains (~115 kDa), the width increased to ~9 nm, whereas the length was unchanged (**Fig. 3c**,**e** and **Supplementary Fig. 3d**). This suggests that the tail domain contributes mainly to the additional density around the head, presumably a result of its binding at this location (appearances of M10tail are shown in **Supplementary Fig. 3c**). Comparison of the averaged images from the constructs allowed us to identify the motor, IQ and tail domains (**Fig. 3e**,**f**).

To confirm these observations, we examined M10full. In low salt with ATP, the majority of M10full were wider molecules (~9 nm; **Fig. 3d**), whereas narrow molecules with head shapes similar to those of M10ΔGTD were seen both in high salt with ATP and in low salt without ATP (**Supplementary Fig. 3a**,**b**). We used single-particle image processing to determine the structural characteristics of these wider molecules, which provided structural evidence for intramolecular interactions between the head and the tail domain. Averaged images of the wider molecules showed many views of closely packed structures of M10full (**Supplementary Fig. 3d**). Averaged images (M10full in **Fig. 3e**) showed that the tail domain folds backward to the head (**Fig. 3f**) so that it appears to interact with the head. With the results of tail-induced inhibition of the actin-activated ATPase activities (**Fig. 2**), this structural information supports a model in which the inhibition of M10full results from an interaction between the head and tail domains.

Phospholipids abolish the tail-induced inhibition

A key question concerns how the motor activity of myosin X that is inhibited by its tail can be activated, as Ca^{2+} did not counteract the inhibition by the tail domain (in contrast to what is seen for myosin Va[15,17–20] and myosin VIIa[16]). We hypothesized that the binding of the tail domain to the cargo molecules attenuates the interaction between the tail and motor domain, thereby releasing the inhibition. Myosin X has a PH domain, which has a PtdIns(3,4,5)P_3-binding consensus sequence (**Supplementary Fig. 6**). As the deletion of the PH domain abolished the tail-dependent inhibition (**Fig. 2c**), we tested whether PtdIns(3,4,5)P_3-containing phospholipids affected the actin-activated ATPase activity of myosin X. A phospholipid overlay assay showed that M10PH-FERM bound to PtdIns(3,4,5)P_3, but not to phosphoinositol or PtdIns(3,4)P_2. It also bound to PtdIns(4,5)P_2 with reduced potency (**Supplementary Fig. 7a**). M10full bound to PtdIns(3,4,5)P_3, suggesting that the head domain did not interfere with the interaction between the tail and PtdIns(3,4,5)P_3 (**Supplementary Fig. 7a**). The actin-activated ATPase activity of M10full was markedly activated by PtdIns(3,4,5)P_3 or PtdIns(4,5)P_2 but was not activated by phosphoinositol or PtdIns(3,4)P_2 (**Fig. 4a**). Consistently, the addition of phospholipids containing PtdIns(3,4,5)P_3 markedly attenuated the tail-induced inhibition of actin-activated ATPase activity in M10ΔGTD (**Fig. 4b**), but not in the absence of the tail (**Fig. 4b**). Control phospholipids without PtdIns(3,4,5)P_3 did not reverse the inhibition of the tail domain (**Fig. 4b**). These results suggest that PtdIns(3,4,5)P_3 interacts with the PH domain of the tail, thereby abolishing the interaction between

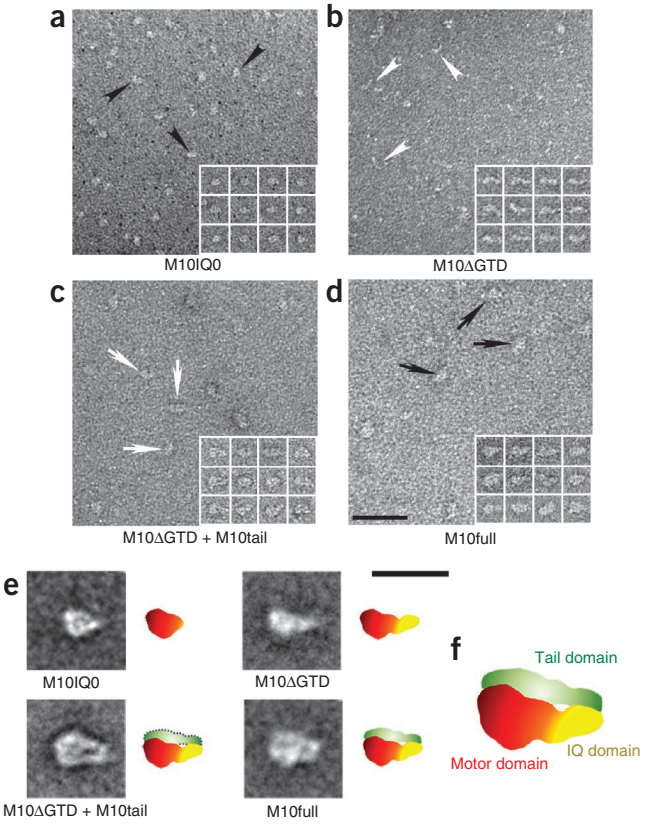

Figure 3 Electron microscopy analysis of myosin X constructs. (**a**,**b**) Negatively stained fields of M10IQ0 and M10ΔGTD. Black and white arrowheads point to individual molecules in each field, appearing as single-headed monomers. (**c**,**d**) Fields of M10ΔGTD with the tail domain and M10full, respectively. White and black arrows indicate appearances of wider molecules observed in fields. Note that ~50% of molecules appeared as closely packed wider molecules as a result of intermolecular interactions between the head and the tail domain, consistent with the results shown in **Figure 2**. Inset images in **a**–**d**, galleries of raw images of individual molecules taken from each construct. (**e**) Selected averages of myosin X constructs chosen on the basis of similar oriented views in each construct; M10IQ0 (upper left), M10ΔGTD (upper right), M10ΔGTD + M10tail construct (lower left) and M10full (lower right). Each average consists of 20–50 images. Adjacent schematic drawings show possible interpretations of densities of each construct identified from the averages. (**f**) Enlarged drawing of M10full showing main domains of closely packed M10full. Electron microscope specimen preparations of all samples (**a**–**d**) were diluted with 50 mM sodium acetate in the presence of ATP. Scale bars, 50 nm (**a**–**d**) and 20 nm (**e**).

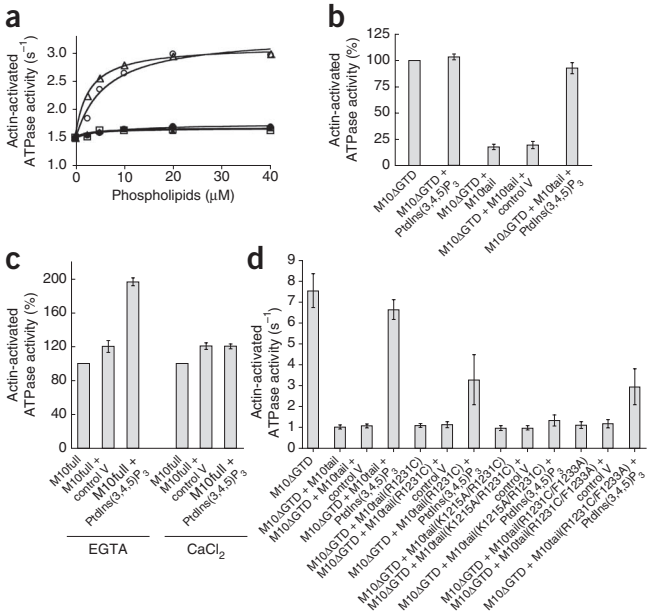

Figure 4 Binding of PtdIns(3,4,5)P_3 to myosin X abolishes the tail-induced inhibition of the actin-activated ATPase activity of myosin X. (**a**) Effect of phospholipid-containing vesicles on the actin-activated ATPase activity of M10full. Open triangles, PtdIns(4,5)P_2; open circles, PtdIns(3,4,5)P_3; closed triangles, PtdIns(3,4)P_2; closed circles, phosphatidylinositol; open squares, control vesicles. Molar ratio composition of each vesicle is 2:6:2 for PtdIns:phosphatidylcholines:phosphatidylserine. Molar ratio of the control vesicle is 8:2 for phosphatidylcholines:phosphatidylserine. (**b**) Reversal of tail-induced inhibition of the actin-activated ATPase activity of M10ΔGTD (0.05 μM) by vesicles containing PtdIns(3,4,5)P_3. We used 0.5 μM M10tail. (**c**) Effect of Ca^{2+} on the PtdIns(3,4,5)P_3-dependent activation of the actin-activated ATPase activity of full-length myosin X (M10full). (**d**) Mutation of PH2 domain in myosin X attenuated the PtdIns(3,4,5)P_3-induced activation of actin-activated ATPase activity of M10ΔGTD in the presence of M10tail. We examined the effect of R1231C, R1231C/K1215A or R1231C/F1233A mutations on the PtdIns(3,4,5)P_3-induced activation of actin-activated ATPase activity of M10ΔGTD (0.05 μM) in the presence of M10tail (0.5 μM). The final concentration of PtdIns(3,4,5)P_3 in vesicles (molar ratio of PtdIns(3,4,5)P_3:PC:PS was 2:6:2) was 40 μM. We used 20 μM actin. Values are mean ± s.e.m. from three independent experiments.

the tail and the motor domain and releasing the tail-induced inhibition. Although Ca^{2+} does not directly influence the tail inhibition, Ca^{2+} abolished the activation of full-length myosin X by PtdIns(3,4,5)P_3 (**Fig. 4c**). The reverse inhibition by PtdIns(3,4,5)P_3 was also attenuated in the presence of Ca^{2+} for M10IQ0 (data not shown). Therefore, the effect of Ca^{2+} is likely to be due to the interaction between Ca^{2+} and phospholipids. A Ca^{2+}-induced change in the structure of phospholipids has been reported[21].

There are three PH domains in the M10tail. The second PH domain (PH2) is the most conserved (**Supplementary Fig. 6**). The phospholipid-binding activity of the PH3 domain was much weaker than that of the PH2 domain (**Supplementary Fig. 7b**). On the other hand, the conserved phenylalanine is absent in PH1, and it is thought that PH1 does not bind phospholipids (**Supplementary Fig. 6**). To support this idea, we produced three mutants, in which the conserved amino acid residues in β1 (Lys1215) or β2 (Arg1231 and Phe1233) in the PH2 domain were mutated (**Supplementary Fig. 6**). Reversal of the M10tail-induced inhibition of the actin-activated ATPase activity of M10ΔGTD by PtdIns(3,4,5)P_3 was attenuated by these mutations (**Fig. 4d**). In the presence of tail, PtdIns(3,4,5)P_3 increased the ATPase activity by 560%, which was reduced to 230% for the R1231C mutant. Additional mutation of K1215A (R1231C/K1215A) further decreased the PtdIns(3,4,5)P_3-induced activation to 30%. Consistently, these mutations attenuated binding of M10tail by PtdIns(3,4,5)P_3 (**Supplementary Fig. 7a**). These results indicate that binding of M10tail by PtdIns(3,4,5)P_3 abolishes the tail-induced inhibition of the actin-activated ATPase activity of myosin X. This presumably occurs as a result of the disruption of the head-tail interaction. Note that the mutation did not alter the tail-induced inhibition of M10ΔGTD in the absence of PtdIns(3,4,5)P_3 (**Fig. 4d**).

PtdIns(3,4,5)P_3 activates motility of myosin X

We examined the effect of PtdIns(3,4,5)P_3 on the motor activity of myosin X with an *in vitro* actin gliding assay (**Fig. 5**). In the presence of PtdIns(3,4,5)P_3, M10full moved actin filaments with a velocity of 0.29 ± 0.09 μm s^{-1} (**Fig. 5b**). This value is comparable to that obtained for the tail-truncated construct (M10ΔGTD)[22]. On the other hand, the velocity of M10full with the control vesicle was much lower. Most actin filaments moved very slowly (0.05 μm s^{-1}), whereas some moved faster (**Fig. 5a**). This result is consistent with the inhibition of the actin-activated ATPase activity by the tail, and it suggests that the tail domain serves as an intramolecular inhibitor of myosin X motor activity and that binding of PtdIns(3,4,5)P_3 to the PH domain in the tail activates the actin gliding activity of M10full. It is likely that the regulation of a certain population of M10full is disrupted as a result of attachment of the molecules to the cover slip, and this may result in unregulated fast actin movement (**Fig. 5a**) for some actin filaments.

A key question is whether myosin X can form a dimer, as myosin X is a high-duty-ratio myosin[7] and it is thought that dimer formation is important for high-duty-ratio myosins to move processively with a hand-over-hand mechanism. The forced dimer can move processively on single actin filaments[10] or actin bundles[10,23]. As myosin X can move to filopodial tips[11,12], we hypothesized that myosin X–binding molecules might facilitate dimer formation and thereby enable myosin X to move processively. As PtdIns(3,4,5)P_3 activates the ATPase activity of myosin X, we examined the effect of PtdIns(3,4,5)P_3 on the formation of myosin X dimers. We subjected the head domain–truncated myosin X (M10tail/CC) to chemical cross-linking followed by SDS-PAGE analysis in the presence or absence of PtdIns(3,4,5)P_3. The high-molecular-mass band of M10tail/CC appeared in the presence of vesicles with but not without PtdIns(3,4,5)P_3 (**Fig. 6a**). Deletion of the predicted coiled-coil domain (M10tail) abolished the

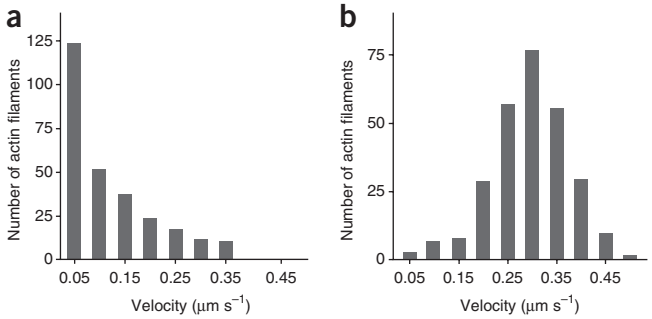

Figure 5 Activation of the actin-gliding velocity of M10full by PtdIns(3,4,5)P_3. (**a**,**b**) We determined the actin-gliding activity of M10full in the presence of control vesicle (molar ratio of 8:2 for diC8-phosphatidylcholine:diC8-phosphatidylserine; **a**) or diC8- PtdIns(3,4,5)P_3 (Echelon; **b**) (see Online Methods). The velocity every 20 s (**a**) or 10 s (**b**) was measured with randomly selected moving actin filaments. The mean ± s.d. values were 0.11 ± 0.09 μm s^{-1} (n = 293) for **a** and 0.29 ± 0.09 μm s^{-1} (n = 286) for **b**.

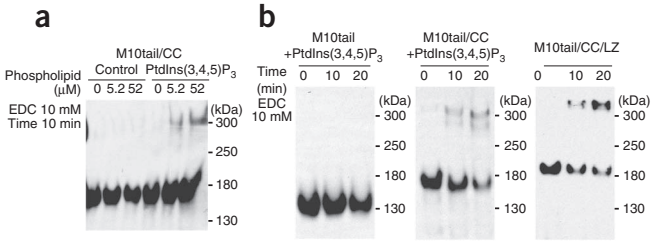

Figure 6 Induction of myosin X dimer formation by PtdIns(3,4,5)P_3 measured by cross-linking. Myc-M10tail/CC or M10tail (10 nM) was subjected to cross-linking with 10 mM EDC for 10 min in the presence of PtdIns(3,4,5)P_3-containing vesicles (molar ratio of PtdIns(3,4,5)P_3: phosphatidylcholine:phosphatidylserine was 2:6:2) or control vesicles (molar ratio of phosphatidylcholine:phosphatidylserine, 8:2). We used M10tail/CC/LZ as a positive control. We analyzed dimer formation by western blot using anti-Myc antibodies. Right, molecular masses. (**a**) Effect of PtdIns(3,4,5)P_3 on dimer formation of M10tail/CC. (**b**) Role of predicted coiled-coil domain in PtdIns(3,4,5)P_3-induced dimer formation.

production of the cross-linked high-molecular-mass band (**Fig. 6b**). M10tail/CC/LZ was cross-linked to form a high-molecular-mass band in the absence of PtdIns(3,4,5)P_3 (**Fig. 6b**). These results suggest that the high-molecular-mass band represents the cross-linked dimer and that the predicted coiled-coil domain promotes the PtdIns(3,4,5)P_3-induced formation of dimers, although this domain by itself does not produce a stable dimer. It is possible that the observed high-molecular-mass cross-linked product might result from the clustering of the molecule on lipid membrane. However, this is less likely because the deletion of the predicted coiled-coil domain eliminated the cross-linked product. These results suggest that the binding of myosin X tail to PtdIns(3,4,5)P_3 not only activates the motor activity but also induces the formation of myosin X dimers.

Figure 7a shows the localization of green fluorescent protein (GFP)–myosin X and its variants in COS7 cells. The localization of M10full(R1231C) in the filopodial tip was much lower than that of M10full (**Fig. 7a**,**b**). M10fullΔMyTH4/FERM showed filopodial tip localization similar to that of M10full, whereas tip localization was notably diminished for M10fullΔPH/MyTH4/FERM lacking the PH domain (**Fig. 7a**,**b**). These results are consistent with *in vitro* findings that PtdIns(3,4,5)P_3 binds to the PH domain and induces dimer formation. Note that the deletion of the predicted coiled coil diminished the tip localization of the myosin X construct, which contains the PH domain. This result is consistent with the cross-linking experiment (**Fig. 6**) and supports the notion that the formation of myosin X dimers

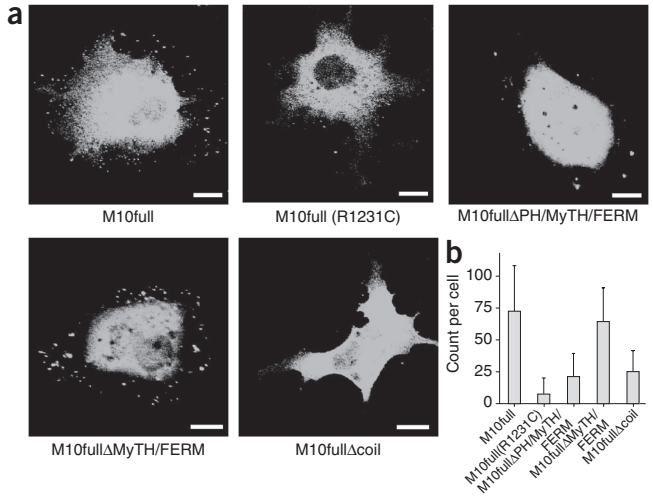

Figure 7 Phospholipid binding is crucial for the filopodial tip localization of myosin X. COS 7 cells were transfected with GFP-M10full, GFP-M10full (R1231C), GFP-M10fullΔPH/MyTH4/FERM, GFP-M10fullΔMyTH4/FERM or M10fullΔcoil. (**a**) Representative images. Scale bars, 10 μm. (**b**) Statistical analysis of the number of filopodia per cell with the tip GFP signal. Values are mean ± s.e.m. (GFP-M10full, $n = 65$; GFP-M10full (R1231C), $n = 30$; GFP-M10fullΔPH/MyTH4/FERM, $n = 23$; GFP-M10fullΔMyTH4/FERM, $n = 24$; M10fullΔcoil, $n = 43$).

is important for its localization at the filopodial tip. This result also suggests that the localization of myosin X at the filopodial tip is not simply due to the binding of myosin X to PtdIns(3,4,5)P_3 at the tips.

DISCUSSION

Tail-dependent inhibition of ATPase activity

A key finding of this study is that the tail domain of myosin X binds to the motor domain and inhibits motor activity in a phospholipid-dependent and Ca^{2+}-independent manner. Electron microscopy analysis provided a structural basis for the tail-induced inhibition of myosin X. Whereas M10full molecules show a closely packed conformation at low ionic strength with ATP (**Supplementary Fig. 3**), they appear unfolded at high ionic strength or at low ionic strength without ATP (**Supplementary Fig. 3**). This is consistent with dependence of the tail-dependent inhibition on ionic strength (**Supplementary Fig. 5**). Single-particle analysis of the closely packed conformation showed an intramolecular interaction between the head and the tail. This structural analysis agrees with the biochemical functional analysis. Our results also suggest that the inhibited conformation requires binding of ATP to the motor domain. As the steady-state intermediate in the absence of actin is M-ADP phosphate[7], it is thought that the formation of the ternary complex (pre–power stroke conformation) is important for the tail to bind to the head and inhibit activity.

On the basis of these findings, we propose the following model for the regulation of myosin X (**Supplementary Fig. 8a**). In physiological ionic conditions, myosin X forms an inhibited conformation, in which the two distinct regions of the tail domain bind to the head to prevent free movement of the myosin head, thus decreasing the ATP hydrolysis cycle rate. It has been shown by us and others that the tail domain inhibits the one-headed *Drosophila* myosin VIIa[16,24]. Although the binding sites responsible for the tail-induced inhibition for myosin X are different from myosin VIIa, this intramolecular interaction—that is, the folding back of the tail onto the head—is a general mechanism for inhibiting single-headed myosins.

Ca^{2+}-independent and phospholipid dependent regulation

Our results indicate that for myosin X, unlike for myosin Va[15,17–20] and myosin VIIa[16], Ca^{2+} does not affect tail-induced inhibition. This is consistent with the fact that the elimination of the calmodulin-associated IQ domain does not abolish the tail-induced inhibition. For myosin VIIa, it has been shown that the distal IQ domains bind the tail[16], whereas for myosin X we have found that the IQ domains are not important for tail-induced inhibition. These findings suggest that the Ca^{2+} sensitivity of the tail-induced inhibition of myosin VIIa results from the tail binding to calmodulin itself or to the adjacent region of the heavy chain, and that the binding of Ca^{2+} to calmodulin abolishes the tail binding. On the other hand, the myosin X tail does not bind the IQ domain, and it presumably interacts directly with the motor head domain.

A key question concerns how the inhibited state of myosin X becomes activated in cells. As the tail domain serves as a cargo-binding domain, we hypothesized that the binding of cargo molecules might

interfere with the interaction between the tail and the motor domain and thereby abolish the inhibition. We found that PtdIns(3,4,5)P_3 bound to the PH domain. This not only reversed the tail-induced inhibition but also induced the formation of myosin X dimers. We propose the following scenario. The region responsible for the dimer formation in the tail is occluded in the inhibited conformation. Binding of PtdIns(3,4,5)P_3 to the PH domain disrupts the tail-head interaction (**Supplementary Fig. 8a**) and abolishes the tail-induced inhibition of the motor activity. The activated conformation is compatible with dimer formation. As dimer formation is crucial for the processive movement of myosin X[10–12,23] by a hand-over-hand mechanism, we conclude that the binding of myosin X to PtdIns(3,4,5)P_3 disrupts the interaction between the tail and the motor domain. This activates the motor activity and dimer formation of myosin X and thereby results in the transport of its cargo complex (**Supplementary Fig. 8b**).

Single-headed structure of full-length myosin X

Our results show that full-length myosin X is a single-headed myosin, as determined by cross-linking (**Supplementary Fig. 2**) and electron microscopy (**Fig. 3** and **Supplementary Fig. 3**). It was previously reported that tail-truncated myosin X, which has a predicted coiled-coil domain, was predominantly monomeric, with approximately 10% dimeric[2]. Our results are consistent with the earlier report and further indicate that the tail domain by itself does not promote dimer formation. Dimer formation is crucial for the processive movement of myosin X *in vitro*[10], whereas the full-length myosin X moves processively within filopodia[11,12]. This finding suggests that the presence of the tail domain is essential for the movement of myosin X and its cargo molecules to filopodial tips, presumably as a result of dimer formation in cells. This apparent discrepancy is solved by the finding that binding of PtdIns(3,4,5)P_3 induces the formation of myosin X dimers. The formation of myosin X dimers is crucial for the initiation of filopodia at the leading edge[25], and we propose that the mechanical activity of the two-headed myosin X is involved in actin filament convergence at the leading edge. PtdIns(3,4,5)P_3 is localized at the cell periphery including the leading edge[26]. Our results suggest that PtdIns(3,4,5)P_3 binds to the myosin X tail and thereby promotes the formation of dimers at the cell periphery. Therefore, we propose the following scenario for the activation of myosin X in cells. The inhibited conformation of the myosin X monomer encounters PtdIns(3,4,5)P_3 at the leading edge of the cell. This induces the conformational change from the inhibited form to the active form (**Supplementary Fig. 8a**). The active conformation of myosin X readily forms a dimer and exerts force to induce the convergence of actin filaments and produce the base of filopodia. The active myosin X dimer moves toward the filopodial tips with its cargo molecules to help in filopodial elongation[12] (**Supplementary Fig. 8b**). Further studies are required to clarify the mechanism of myosin X function in the formation of filopodia.

METHODS

Methods and any associated references are available in the online version of the paper at http://www.nature.com/nsmb/.

Note: Supplementary information is available on the Nature Structural & Molecular Biology website.

ACKNOWLEDGMENTS

We thank R. Fenton (University of Massachusetts) for reading the manuscript and K. Homma for the parent construct of myosin X. This work was supported by US National Institutes of Health (NIH) grants DC006103, AR048526, AR048898 and HL073050 to M.I. and Korea Basic Science Institute grant T31760 to H.S.J.

AUTHOR CONTRIBUTIONS

N.U. performed the ATPase assays of myosin X constructs, cross-linking assay and prepared myosin X proteins for EM experiments. H.S.J. performed EM image analysis and wrote the EM part of the paper. T.S. performed lipid binding assay, cross-linking, cell imaging, measurement of the activity of PH domain mutants and production of some myosin X constructs. O.S. performed the actin gliding assay of myosin X. R.I. prepared myosin X expression constructs. M.I. supervised the whole project and wrote the paper.

COMPETING FINANCIAL INTERESTS

The authors declare no competing financial interests.

Published online at http://www.nature.com/nsmb/.
Reprints and permissions information is available online at http://www.nature.com/reprints/index.html.

1. Berg, J.S., Derfler, B.H., Pennisi, C.M., Corey, D.P. & Cheney, R.E. Myosin-X, a novel myosin with pleckstrin homology domains, associates with regions of dynamic actin. *J. Cell Sci.* **113**, 3439–3451 (2000).
2. Knight, P.J. *et al.* The predicted coiled-coil domain of myosin 10 forms a novel elongated domain that lengthens the head. *J. Biol. Chem.* **280**, 34702–34708 (2005).
3. Tokuo, H. & Ikebe, M. Myosin X transports Mena/VASP to the tip of filopodia. *Biochem. Biophys. Res. Commun.* **319**, 214–220 (2004).
4. Zhang, H. *et al.* Myosin-X provides a motor-based link between integrins and the cytoskeleton. *Nat. Cell Biol.* **6**, 523–531 (2004).
5. Weber, K.L., Sokac, A.M., Berg, J.S., Cheney, R.E. & Bement, W.M. A microtubule-binding myosin required for nuclear anchoring and spindle assembly. *Nature* **431**, 325–329 (2004).
6. Homma, K., Saito, J., Ikebe, R. & Ikebe, M. Motor function and regulation of myosin X. *J. Biol. Chem.* **276**, 34348–34354 (2001).
7. Homma, K. & Ikebe, M. Myosin X is a high duty ratio motor. *J. Biol. Chem.* **280**, 29381–29391 (2005).
8. Ikebe, M. Regulation of the function of mammalian myosin and its conformational change. *Biochem. Biophys. Res. Commun.* **369**, 157–164 (2008).
9. Kolomeisky, A.B. & Fisher, M.E. Molecular motors: a theorist's perspective. *Annu. Rev. Phys. Chem.* **58**, 675–695 (2007).
10. Sun, Y. *et al.* Single-molecule stepping and structural dynamics of myosin X. *Nat. Struct. Mol. Biol.* **17**, 485–491 (2010).
11. Kerber, M.L. *et al.* A novel form of motility in filopodia revealed by imaging myosin-X at the single-molecule level. *Curr. Biol.* **19**, 967–973 (2009).
12. Watanabe, T.M., Tokuo, H., Gonda, K., Higuchi, H. & Ikebe, M. Myosin-X induces filopodia by multiple elongation mechanism. *J. Biol. Chem.* **285**, 19605–19614 (2010).
13. Berg, J.S. & Cheney, R.E. Myosin-X is an unconventional myosin that undergoes intrafilopodial motility. *Nat. Cell Biol.* **4**, 246–250 (2002).
14. Sousa, A.D., Berg, J.S., Robertson, B.W., Meeker, R.B. & Cheney, R.E. Myo10 in brain: developmental regulation, identification of a headless isoform and dynamics in neurons. *J. Cell Sci.* **119**, 184–194 (2006).
15. Li, X.D., Jung, H.S., Mabuchi, K., Craig, R. & Ikebe, M. The globular tail domain of myosin Va functions as an inhibitor of the myosin Va motor. *J. Biol. Chem.* **281**, 21789–21798 (2006).
16. Umeki, N. *et al.* The tail binds to the head-neck domain, inhibiting ATPase activity of myosin VIIA. *Proc. Natl. Acad. Sci. USA* **106**, 8483–8488 (2009).
17. Wang, F. *et al.* Regulated conformation of myosin V. *J. Biol. Chem.* **279**, 2333–2336 (2004).
18. Li, X.D., Mabuchi, K., Ikebe, R. & Ikebe, M. Ca2+-induced activation of ATPase activity of myosin Va is accompanied with a large conformational change. *Biochem. Biophys. Res. Commun.* **315**, 538–545 (2004).
19. Li, X.D. *et al.* The globular tail domain puts on the brake to stop the ATPase cycle of myosin Va. *Proc. Natl. Acad. Sci. USA* **105**, 1140–1145 (2008).
20. Krementsov, D.N., Krementsova, E.B. & Trybus, K.M. Myosin V: regulation by calcium, calmodulin, and the tail domain. *J. Cell Biol.* **164**, 877–886 (2004).
21. Levental, I. *et al.* Calcium-dependent lateral organization in phosphatidylinositol 4,5-bisphosphate (PIP2)- and cholesterol-containing monolayers. *Biochemistry* **48**, 8241–8248 (2009).
22. Homma, K., Yoshimura, M., Saito, J., Ikebe, R. & Ikebe, M. The core of the motor domain determines the direction of myosin movement. *Nature* **412**, 831–834 (2001).
23. Nagy, S. *et al.* A myosin motor that selects bundled actin for motility. *Proc. Natl. Acad. Sci. USA* **105**, 9616–9620 (2008).
24. Yang, Y. *et al.* A FERM domain autoregulates *Drosophila* myosin 7a activity. *Proc. Natl. Acad. Sci. USA* **106**, 4189–4194 (2009).
25. Tokuo, H., Mabuchi, K. & Ikebe, M. The motor activity of myosin-X promotes actin fiber convergence at the cell periphery to initiate filopodia formation. *J. Cell Biol.* **179**, 229–238 (2007).
26. Sasaki, A.T., Chun, C., Takeda, K. & Firtel, R.A. Localized Ras signaling at the leading edge regulates PI3K, cell polarity, and directional cell movement. *J. Cell Biol.* **167**, 505–518 (2004).

ONLINE METHODS

Cloning and expression of myosin X constructs. Bovine myosin X cDNA was obtained as described[6,7]. The amino acid sequence matches the submitted *Myo10* gene sequence (GenBank accession no. NM_174394). The cDNA fragment encoding M10full was subcloned into pFastBacHT baculovirus vector containing a Flag tag sequence at the 5′ end. C-terminally truncated myosin X constructs were produced by introducing a stop codon at various sites in M10full (**Fig. 1**). N-terminally truncated M10tail was constructed by PCR and subcloned into pFastBacHT vector. M10M5cc was produced by fusing M10ΔGTD (amino acids 1–939) with the myosin V coiled-coil domain (amino acids 908–1,090 of mouse myosin Va). An NheI site was created at nucleotide 2,817 of M10ΔGTD and the cDNA fragment of the mouse myosin V gene (GenBank accession no. NM_010864) encoding amino acids 908–1,090 flanked with NheI sites was introduced into M10ΔGTD. The NheI site was then mutated to restore the original amino acids. M10full LZ was produced by fusing M10full with the GCN4 leucine zipper at the C-terminal end of M10full. An NheI site was created at the end of the coding sequence and GCN4 flanked with NheI sites was introduced. For the multimolecule *in vitro* motility assay, the cDNA sequence of M10full was inserted into pFastBacHT vector having c-Myc and Flag sequences using a Mlu1 site created at the 3′ end of M10full.

Myosin X constructs were expressed in Sf9 cells and were purified using anti-Flag resin[7,10]. The purified myosin X samples were dialyzed against 30 mM HEPES-KOH, pH 7.5, 300 mM KCl, 2 mM $MgCl_2$, 0.2 mM EGTA, 1 mM dithiothreitol and 10% (w/v) sucrose. The concentration of myosin X samples was determined as described[6]. M10PH2 and M10PH3 domains were produced by PCR, subcloned into the pGEX vector to make GST-PH2 and GST-PH3 constructs, and expressed in *Escherichia coli*. The proteins were purified using glutathione–Sepharose 4B resin. Myosin X constructs were also subcloned into pEGFPC1 vector for cell localization studies. The C-terminally deleted GFP–myosin X constructs were generated by introducing a stop codon at appropriate sites. For M10fullΔcoil, a set of unique restriction enzyme sites (HindIII) were created, and the cDNA fragment encoding the coil was excised.

Steady-state ATPase assay. The steady-state ATPase activity was measured in buffer containing 0.05–0.1 μM myosin X, 20 μM actin, 1 mM ATP, 30 mM HEPES-KOH, pH 7.5, 30 mM KCl, 2 mM $MgCl_2$, 1 mM DTT, 15 μg ml^{-1} calmodulin, 1 mM EGTA-$CaCl_2$ buffer system in the presence of ATP regeneration system (20 units ml^{-1} pyruvate kinase and 2 mM phosphoenolpyruvate) at 25 °C. The reaction solution was mixed and preincubated at 25 °C for 10 min before adding ATP to start the reaction, and the ATPase activity was determined by measuring liberated pyruvate as described[27].

EDC cross-linking. M10ΔGTD, M10M5cc, M10full and M10full LZ (all 0.02 mg ml^{-1}) were incubated with 50 mM EDC (1-ethyl-3-(3-dimethylaminopropyl)carbodiimide) (Sigma), 300 mM NaCl, 30 mM HEPES-KOH pH 7.5, 1 mM EGTA, 30 μg ml^{-1} calmodulin, 0.5% (v/v) Triton X-100, 2 mM ATP and 1 mM $MgCl_2$ for the indicated time at 25 °C (**Supplementary Fig. 2**). M10tail/CC, M10tail and M10tail/CC/LZ (all 10 nM) were incubated with 10 mM EDC, 150 mM NaCl, 30 mM HEPES-KOH, pH 7.5, 2 mM ATP, 1 mM $MgCl_2$ and 1 mM EGTA for 10 min at 25 °C (**Fig. 6**). The reactions were terminated by addition of 70 mM Tris-HCl pH 6.8, 50 mM dithiothreitol. The cross-linking products were analyzed by western blot using anti-Flag antibodies (**Supplementary Fig. 2**) or anti-Myc antibodies (**Fig. 6**) as described[28].

***In vitro* motility assay.** The *in vitro* actin gliding assay was conducted as described[7]. The movement of the rhodamine-labeled actin filaments was observed in the motility assay buffer (25 mM KCl, 25 mM HEPES (pH 7.5), 5 mM $MgCl_2$, 1 mM EGTA, 1% (v/v) 2-mercaptethanol, 36 μg ml^{-1} catalase, 4.5 mg ml^{-1} glucose, 216 μg ml^{-1} glucose oxidase, 5 μM calmodulin and 2 mM MgATP) at 25 °C. The anti–c-Myc antibody (Santa Cruz) was used to attach M10full with C-terminal Myc tag to coverslips. The antibody was first introduced to a flow cell to attach to the surface of a coverslip. After the flow cell was blocked with 1 mg ml^{-1} BSA, M10full (~0.05 mg ml^{-1}) was introduced into the flow cell and incubated for 5 min. ATP and rhodamine-labeled actin filaments in the motility assay buffer were then added to the flow cell. The movement of actin filaments was observed with a fluorescence microscope (Olympus IX71), and actin filament velocity was calculated from the movement distance and the elapsed time in successive snapshots.

Electron microscopy and image processing. For negative staining, M10IQ0, M10ΔGTD or M10full (300 nM) was mixed with 6 μM or 3 μM of calmodulin (CaM) for enhancing CaM binding to the myosin X constructs and then diluted ten-fold with low- and high-salt buffer containing 50 mM or 500 mM sodium acetate, 1 mM EGTA, 2 mM $MgCl_2$, 10 mM MOPS and 100 μM ATP, pH 7.5. After dilution, 5 μl of the final mixture was applied to a carbon-coated grid that had been glow-discharged (Harrick Plasma) for 3 min in air, and the grid was immediately (~5 s) negatively stained using 1% (w/v) uranyl acetate[29]. The same procedure was used for the specimens (M10ΔGTD+M10tail construct; initially mixed with low-salt buffer to give the protein concentration of 250 nM in both) made by mixing above final mixture (30 nM M10ΔGTD and 600 (300) nM CaM) with ~300 (30) nM M10tail fragments. At these two molecular ratios of M10ΔGTD and the tail construct, the binding ratio is almost 50% in both. EM grids were examined in a Technai G2 Spirit Twin TEM (FEI) operated at 120 kV, and images were recorded at a magnification of 65,000 (0.37 nm per pixel). Single-particle image processing was carried out using SPIDER (Health Research Inc.) as described in the instructions[30]. Averaged images were produced by alignment and classification of windowed particles (80 × 80 pixels) from micrographs: 1,103 particles (M10IQ0), 786 particles (M10ΔGTD), 788 particles (M10ΔGTD+M10tail fragments) and 671 particles (M10full). Representative averages showing the clearest views of the structures were selected from 20–50 total class averages.

27. Reynard, A.M., Hass, L.F., Jacobsen, D.D. & Boyer, P.D. The correlation of reaction kinetics and substrate binding with the mechanism of pyruvate kinase. *J. Biol. Chem.* **236**, 2277–2283 (1961).
28. Spudich, G. *et al.* Myosin VI targeting to clathrin-coated structures and dimerization is mediated by binding to Disabled-2 and PtdIns(4,5)P2. *Nat. Cell Biol.* **9**, 176–183 (2007).
29. Jung, H.S., Komatsu, S., Ikebe, M. & Craig, R. Head-head and head-tail interaction: a general mechanism for switching off myosin II activity in cells. *Mol. Biol. Cell* **19**, 3234–3242 (2008).
30. Burgess, S.A., Walker, M.L., Thirumurugan, K., Trinick, J. & Knight, P.J. Use of negative stain and single-particle image processing to explore dynamic properties of flexible macromolecules. *J. Struct. Biol.* **147**, 247–258 (2004).